



*Supplement of*

## **Deriving cropland N<sub>2</sub>O emissions from space-based NO<sub>2</sub> observations**

**Taylor J. Adams et al.**

*Correspondence to:* Taylor J. Adams ([adamsta@umich.edu](mailto:adamsta@umich.edu)) and Eric A. Kort ([eric.kort@mpic.de](mailto:eric.kort@mpic.de))

The copyright of individual parts of the supplement might differ from the article licence.

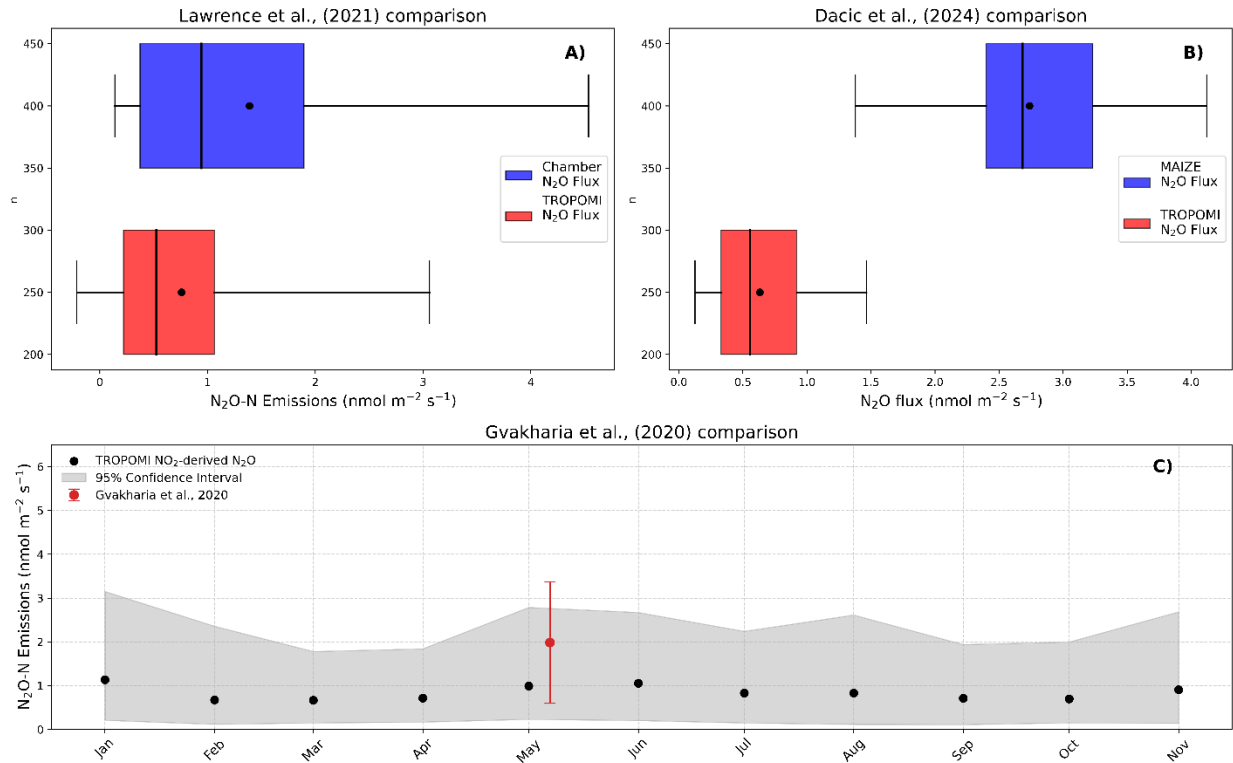


Figure S1: Variation of Figure 3, with a slow (7 hour)  $NO_x$  lifetime. Satellite derived estimates concurrence with independent studies. (A, top left) Box plots of the distribution of daily average  $N_2O$  flux derived from chamber observations detailed in Lawrence et al., 2021 and TROPOMI observations from that period. (B, top right) Box plots of  $N_2O$  flux observed by TROPOMI across the MAIZE campaign domain, and ensemble averages for coincident days of the MAIZE (2021-2022) campaign. (C, Bottom) TROPOMI- $NO_2$  derived  $N_2O$  flux (gray distribution) compared against the  $N_2O$  flux estimate from Gvakharia et al., (2020) (red band).

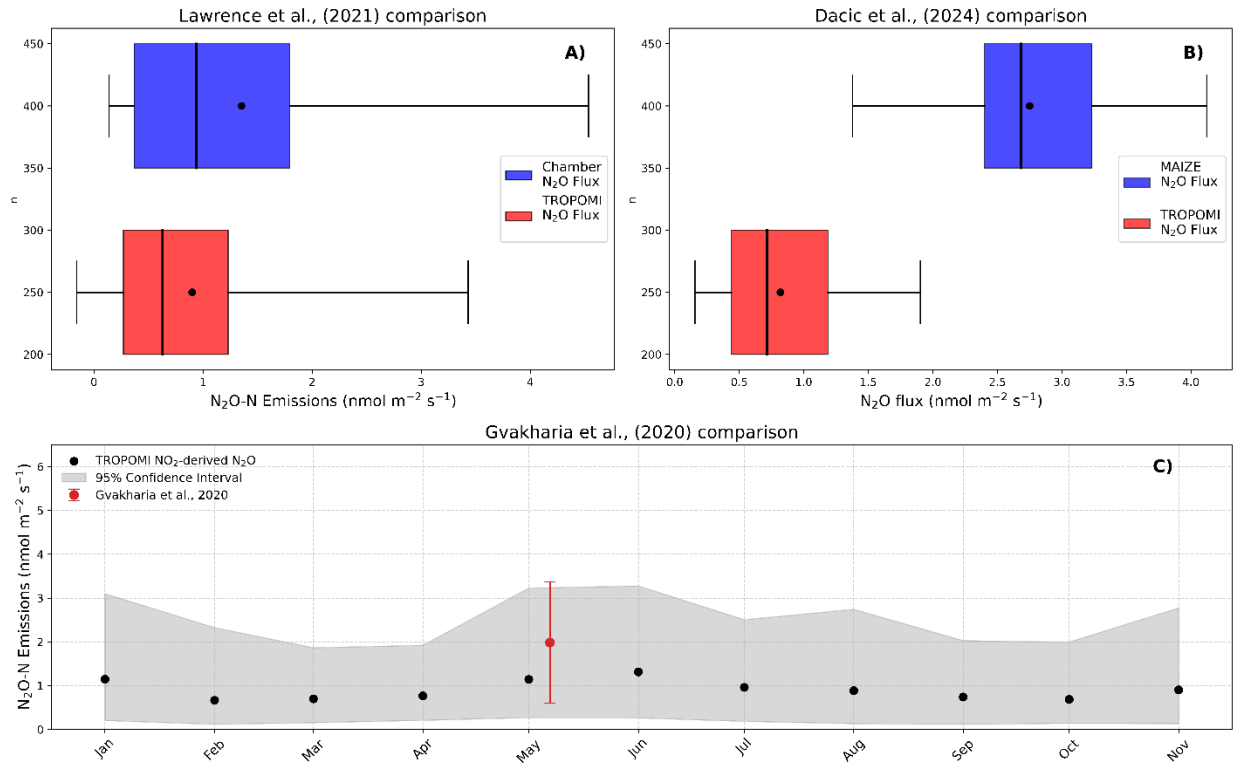


Figure S2: Variation of Figure 3, with a moderate (5 hour) NO<sub>x</sub> lifetime. Satellite derived estimates concurrence with independent studies. (A, top left) Box plots of the distribution of daily average N<sub>2</sub>O flux derived from chamber observations detailed in Lawrence et al., 2021 and TROPOMI observations from that period. (B, top right) Box plots of N<sub>2</sub>O flux observed by TROPOMI across the MAIZE campaign domain, and ensemble averages for coincident days of the MAIZE (2021-2022) campaign. (C, Bottom) TROPOMI-NO<sub>2</sub> derived N<sub>2</sub>O flux (gray distribution) compared against the N<sub>2</sub>O flux estimate from Gvakharia et al., (2020) (red band).

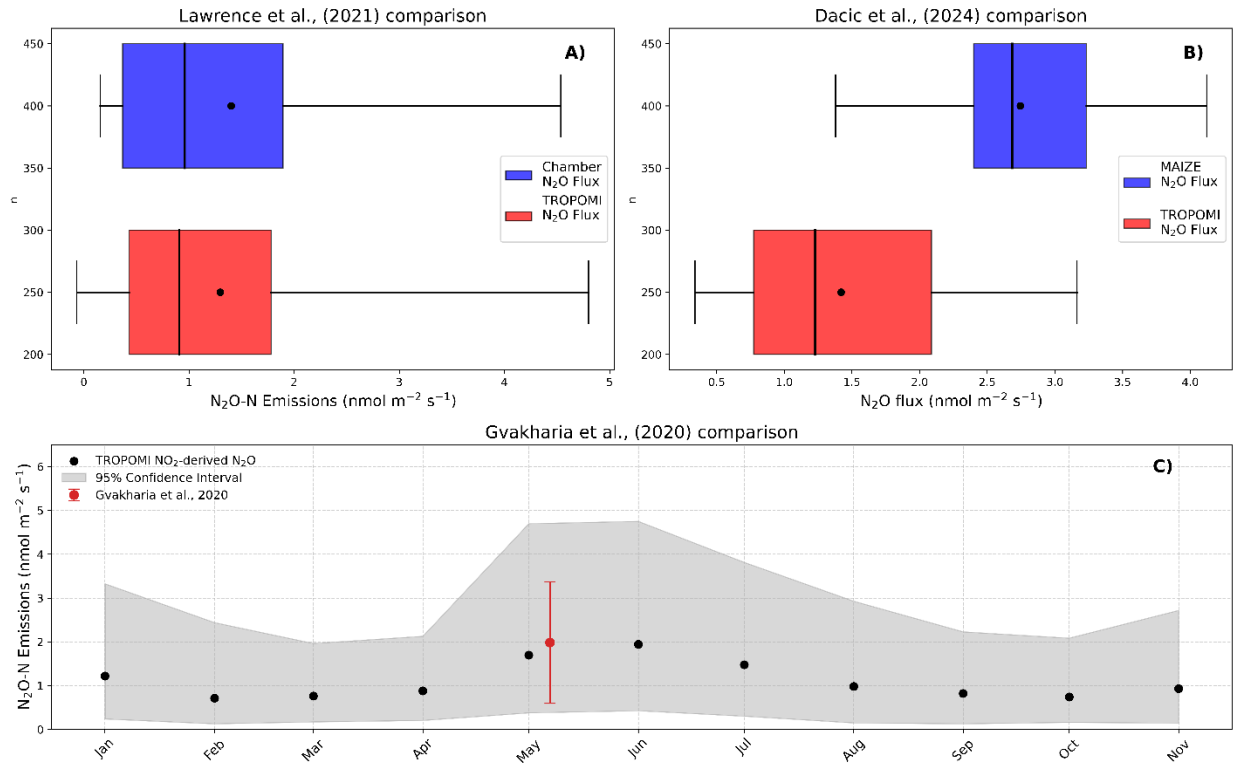


Figure S3: Variation of Figure 3, with a slow (half of main text) deposition rates. Satellite derived estimates concurrence with independent studies. (A, top left) Box plots of the distribution of daily average N<sub>2</sub>O flux derived from chamber observations detailed in Lawrence et al., 2021 and TROPOMI observations from that period. (B, top right) Box plots of N<sub>2</sub>O flux observed by TROPOMI across the MAIZE campaign domain, and ensemble averages for coincident days of the MAIZE (2021-2022) campaign. (C, Bottom) TROPOMI-NO<sub>2</sub> derived N<sub>2</sub>O flux (gray distribution) compared against the N<sub>2</sub>O flux estimate from Gvakharia et al., (2020) (red band).

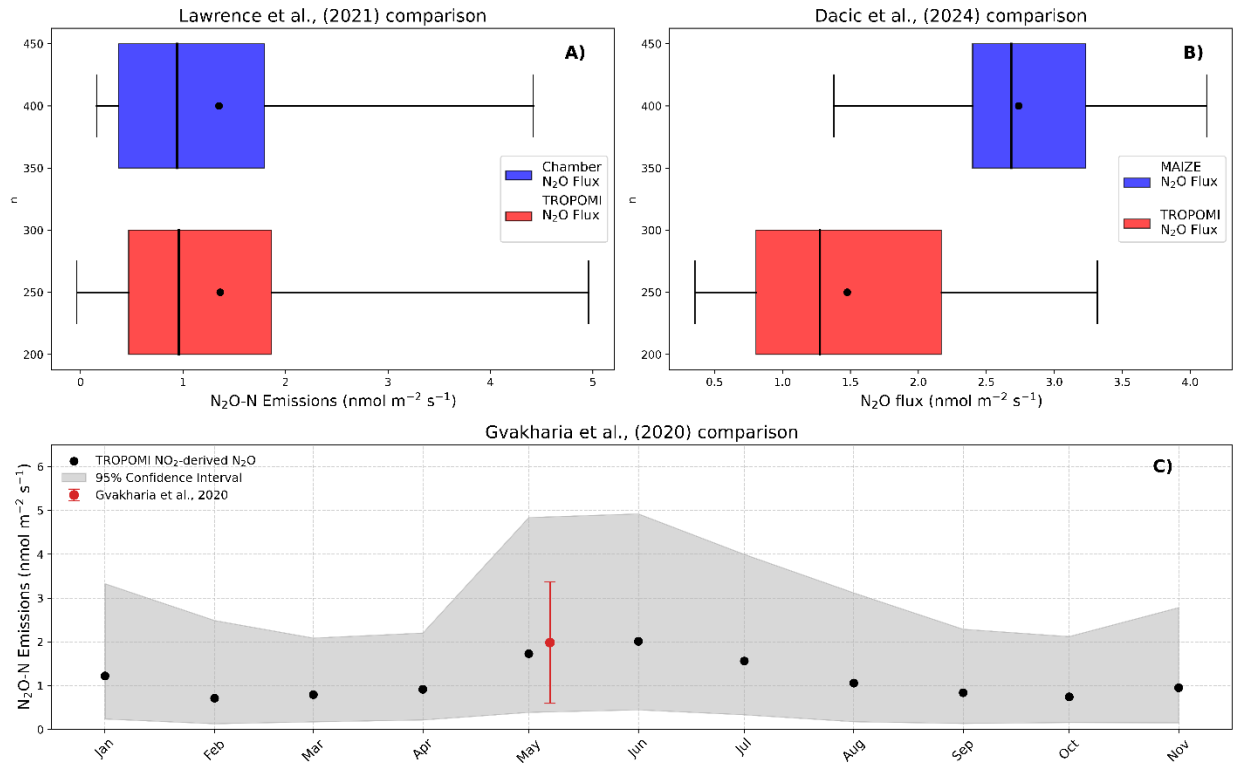


Figure S4: Variation of Figure 3, with a fast (double of main text) deposition rates. Satellite derived estimates concurrence with independent studies. (A, top left) Box plots of the distribution of daily average  $N_2O$  flux derived from chamber observations detailed in Lawrence et al., 2021 and TROPOMI observations from that period. (B, top right) Box plots of  $N_2O$  flux observed by TROPOMI across the MAIZE campaign domain, and ensemble averages for coincident days of the MAIZE (2021-2022) campaign. (C, Bottom) TROPOMI- $NO_2$  derived  $N_2O$  flux (gray distribution) compared against the  $N_2O$  flux estimate from Gvakharia et al., (2020) (red band).